British Journal of Pharmacology (1998) 123, 463–472

State-dependent NMDA receptor antagonism by Ro 8-4304, a novel NR2B selective, non-competitive, voltage-independent antagonist

James N.C. Kew, Gerhard Trube & [1]John A. Kemp

Pharma Division, Preclinical CNS Research, F. Hoffmann-La Roche Ltd, CH-4070 Basel, Switzerland

1 Subunit-selective blockade of N-methyl-D-aspartate (NMDA) receptors provides a potentially attractive strategy for neuroprotection in the absence of undesirable side effects. Here, we describe a novel NR2B-selective NMDA antagonist, 4-{3-[4-(4-fluoro-phenyl)-3,6-dihydro-2H-pyridin-1-yl]-2-hydroxy-propoxy}-benzamide (Ro 8-4304), which exhibits >100 fold higher affinity for recombinant $NR1_{001}$/NR2B than $NR1_{001}$/NR2A receptors.

2 Ro 8-4304 is a voltage-independent, non-competitive antagonist of NMDA receptors in rat cultured cortical neurones and exhibits a state-dependent mode of action similar to that described for ifenprodil.

3 The apparent affinity of Ro 8-4304 for the NMDA receptor increased in an NMDA concentration-dependent manner so that Ro 8-4304 inhibited 10 and 100 μM NMDA responses with IC_{50}s of 2.3 and 0.36 μM, respectively. Currents elicited by 1 μM NMDA were slightly potentiated in the presence of 10 μM Ro 8-4304, and Ro 8-4304 binding slowed the rate of glutamate dissociation from NMDA receptors.

4 These results were predicted by a reaction scheme in which Ro 8-4304 exhibits a 14 and 23 fold higher affinity for the activated and desensitized states of the NMDA receptor, respectively, relative to the agonist-unbound resting state. Additionally, Ro 8-4304 binding resulted in a 3–4 fold increase in receptor affinity for glutamate site agonists.

5 Surprisingly, whilst exhibiting a similar affinity for NR2B-containing NMDA receptors as ifenprodil, Ro 8-4304 exhibited markedly faster kinetics of binding and unbinding to the NMDA receptor. This spectrum of kinetic behaviour reveals a further important feature of this emerging class of NR2B-selective compounds.

Keywords: NMDA receptor antagonists; neuroprotection; glutamate receptors

Introduction

N-methyl-D-aspartate (NMDA) receptor over activation is thought to play a pivotal role in ischaemia-induced neurodegeneration. A wide variety of NMDA receptor antagonists have been identified that act at several different sites on the receptor which afford protection in *in vivo* models of cerebral ischaemia (Kemp & Kew, 1998). Although the neuroprotective ability of many of these compounds is well established, many exhibit associated side effects or lack of efficacy at tolerable dosing levels which has prevented their clinical development (Kemp & Kew, 1998).

Native NMDA receptors are believed to be heteromeric assemblies containing NMDAR1 subunits together with one or more of the four NR2 subunits (NR2A-D) in a pentameric assembly of uncertain stoichiometry (Kutsuwada *et al*., 1992; Monyer *et al*., 1992; Meguro *et al*., 1992; Behe *et al*., 1995; Ferrer-Montiel & Montal, 1996). Nine splice variants of NMDAR1 have been identified including one truncated form that is unable to generate a functional receptor (reviewed by McBain & Mayer, 1994). NMDAR1 splice variants exhibit both distinct expression patterns and functional properties (Laurie & Seeburg, 1994; Laurie *et al*., 1995; Zukin & Bennett, 1995). Similarly, the NR2 subunits, of which splice variants have only been described to date for NR2D, are expressed in a distinct spatio-temporal manner and confer distinct functional properties on heteromeric receptors (reviewed by McBain & Mayer, 1994).

One approach to the problem of preventing NMDA receptor over activation whilst permitting sufficient normal glutamatergic function to avoid unacceptable side effects has been the development of NMDA receptor subunit-selective compounds. In the adult forebrain the predominant NR2 subunits are NR2A and NR2B, with NR2C expressed largely in the cerebellum and various select nuclei, and NR2D expression confined to the diencephalon and midbrain (Kutsuwada *et al*., 1992; Monyer *et al*., 1992; 1994; Ishii *et al*., 1993). Thus, in the adult forebrain the most abundant heteromeric combinations are likely to be NMDAR1/NR2A and NMDAR1/NR2B although a number of recent studies have suggested that NMDAR1/NR2A/NR2C (Wafford *et al*., 1993; Chazot *et al*., 1994) and NMDAR1/NR2A/NR2B (Sheng *et al*., 1994; Luo *et al*., 1997) receptors can exist. Several compounds that appear to discriminate between NMDA receptors composed of different subunit combinations have been described, the best characterized of which is ifenprodil (Williams, 1993; Williams *et al*., 1993; Priestley *et al*., 1994; Kew *et al*., 1996). Ifenprodil is an atypical non-competitive antagonist that was originally believed to interact with the polyamine binding site of the NMDA receptor (Carter *et al*., 1990). However, accumulating evidence suggests that it binds to a distinct site (Reynolds & Miller, 1989; Gallagher *et al*., 1996), although it seems likely that the two binding sites exhibit at least an allosteric linkage (Williams *et al*., 1995; Kashiwagi *et al*., 1996). Ifenprodil exhibits approximately 400 fold higher affinity for NMDAR1-1a/NR2B than for NMDAR1-1a/NR2A hetero-

[1] Author for correspondence.

meric receptors (Williams, 1993) and is neuroprotective both *in vitro* (Graham *et al*., 1992) and in *in vivo* models of cerebral ischaemia (Gotti *et al*., 1988). Notably, ifenprodil lacks many of the side effects exhibited by other NMDA receptor antagonists *in vivo* (Jackson & Sanger, 1988; Perrault *et al*., 1989).

We have recently characterized the mechanism of NMDA receptor antagonism by ifenprodil and have found that it acts by a novel activity-dependent mechanism (Kew *et al*., 1996). This novel mechanism of NMDA receptor antagonism, together with the subunit selectivity, probably contributes to its attractive *in vivo* neuropharmacological profile. Here, we describe a novel NR2B-selective NMDA receptor antagonist, 4-{3-[4-(4-fluoro-phenyl)-3,6-dihyro-2H-pyridin-1-yl]-2-hydroxy-propoxy}-benzamide (Ro 8-4304), which acts by an 'ifenprodil-like' mechanism of activity-dependent NMDA receptor antagonism whilst also exhibiting markedly faster kinetics of receptor binding and unbinding.

Methods

Xenopus *oocyte recordings*

cDNA clones coding for the subunits $NR1_{001}$ (other nomenclature: NR1C or NMDAR1-2a) and NR2A of the NMDA receptor were isolated from a rat brain λgt11 cDNA library as published elsewhere (Sigel *et al*., 1994). The clone for the subunit NR2B of the rat brain NMDA receptor was kindly provided by Dr S. Nakanishi (Kyoto, Japan). The cDNAs were subcloned into the expression vector pBC/CMV, placing transcription of the cDNA under control of the human cytomegalovirus promoter CMV (Bertocci *et al*., 1991). CsCl-purified expression plasmids were mixed in a 1:3 ratio of NR1:NR2 in injection buffer (NaCl 88 mM, KCl 1 mM, HEPES 15 mM, pH 7.0). Oocytes of maturation stage V to VI of South African frogs (*Xenopus laevis*) were used to express the NMDA receptor subunit combinations. Six to 400 pg of the respective cDNA mixture were injected into the nucleus of every oocyte as described, e.g. by Bertrand *et al*. (1991). During the voltage clamp experiments on the following two days, the oocytes were superfused by modified Ringer solution containing NaCl 90 mM, KCl 1 mM, $BaCl_2$ 1 mM and HEPES 5 mM (pH 7.4, 22°C). The membrane potential was held at −80 mV by a 2-microelectrode voltage-clamp circuit (NPI Turbo Tec 05) and the receptors were activated by applying the co-agonists L-glutamate and glycine at concentrations corresponding to their EC_{50}s for the respective subunit combination ($NR1_{001}$ + NR2A: Glu 2.7 μM, Gly 0.9 μM, $NR1_{001}$ + NR2B: Glu 1.3 μM, Gly 0.07 μM). The agonists were applied for 15 s intervals once every 2.5 min by rapidly superfusing the oocyte with agonist containing solution and the amplitude of the evoked current was measured immediately before the end of each application. After a series of initial control stimuli, increasing concentrations of Ro 8-4304 were added to both the basal Ringer and the agonist containing solution. Ro 8-4304 was prepared as a stock solution of 30 mM in DMSO. Due to its limited solubility this was the maximum concentration attainable. Working Ro 8-4304 solutions contained a maximum of 0.1% DMSO, a concentration of DMSO established to exert no independent effects on both *Xenopus* oocytes and cultured cortical neurones. For every oocyte the current amplitudes in the presence of the compound were expressed as a percentage (I) of the control current measured before its application. The function

$$I = (100 - \mathrm{ss})/(1 + (\mathrm{x}/\mathrm{IC}_{50})^{\mathrm{n_H}}) + \mathrm{ss} \qquad \text{(equation 1)}$$

was fitted to the data to estimate the IC_{50} of Ro 8-4304, the Hill coefficient (n_H) and the percentage remaining current (ss).

Cortical neuronal culture

Cortical neurones were prepared from 17-to-18 day-old rat embryos and were grown on astrocyte feeder layers as previously described for hippocampal neurones (Möckel & Fischer, 1994).

Whole-cell voltage-clamp recordings

Cortical neurones were used for electrophysiological experiments after 10–14 days *in vitro*. Whole-cell voltage clamp recordings were performed as described previously (Kew *et al*., 1996) at a holding potential of −60 mV unless stated otherwise.

Exponential curve fitting and measurement of drug on- and off- rates

Neuronal currents were filtered (cut-off frequency, 5 kHz), digitized with a Digidata 1200 (Axon Instruments) and captured on-line to the hard disk of Gateway 2000 P4D-66 Computer using pCLAMP6 software (Axon Instruments). Monoexponential curves were fitted by pCLAMP. Apparent antagonist dissociation constants (K_D) were calculated from measured on- (τ_{on}) and off- (τ_{off}) rate time constants by first deriving the estimated forward (k_+) and reverse (k_-) rate binding constants according to the scheme:

$$\mathrm{R} + \mathrm{A} \underset{k_-}{\overset{k_+}{\rightleftharpoons}} \mathrm{RA} \qquad \text{(equation 2)}$$

Where R is the receptor, A is the antagonist and RA is the antagonist-bound receptor. k_- is the measured $1/\tau_{off}$ and k_+ was derived from the following function:

$$k_+ = (1/\ _{\mathrm{on}} - k_-)/[\mathrm{antagonist}] \qquad \text{(equation 3)}$$

and

$$K_D = k_-/k_+ \qquad \text{(equation 4)}$$

Equilibrium concentration-response curves

Best fit lines were computed for equilibrium concentration-response data for NMDA by use of a two-equivalent binding site model:

$$I = I_{max}/(1 + (\mathrm{m}K_D/[\mathrm{A}]))^2 \qquad \text{(equation 5)}$$

where mK_D is the microscopic dissociation constant and [A] = agonist concentration.

Drugs

N-methyl-D-aspartate (NMDA) and glutamate were obtained from Sigma. Glycine was obtained from Fluka. 4-{3-[4-(4-Fluoro-phenyl)-3,6-dihydro-2H-pyridin-1-yl]-2-hydroxy-propoxy}-benzamide (Ro 8-4304) was synthesized at Hoffmann-La Roche (Basel, Switzerland) and was prepared as a stock solution (30 mM) in dimethyl sulfoxide (DMSO) (Fluka).

Statistical analysis

Data were analysed by paired or unpaired two-tailed t tests as appropriate. Values were considered significant at the $P < 0.05$

level. Mean data are expressed as mean of n experiments ± s.e.mean.

Results

Ro 8-4304 is an NR2B selective NMDA receptor antagonist

The NMDA receptor subunit selectivity of Ro 8-4304 (Figure 1) was investigated by comparing its ability to inhibit currents activated by the co-application of glutamate and glycine to *Xenopus* oocytes expressing recombinant NMDA receptors containing either the NR2A or NR2B subunit together with $NR1_{001}$. Inhibition curves performed with Ro 8-4304 against currents evoked by EC_{50} concentrations of the co-agonists glutamate and glycine at the respective subunit combination yielded an IC_{50} value for NR2B-containing receptors of 0.4 μM (Figure 2b, c). Due to the limited solubility of Ro 8-4304 it was not possible to test concentrations greater than 30 μM. At 30 μM, Ro 8-4304 inhibited only approximately 20% of the control current evoked at NR2A-containing receptors (Figure 2a,c) and, thus, it was not possible to determine an IC_{50} value. However, from these results it is apparent that Ro 8-4304 exhibits >100 fold higher affinity for recombinant NMDA receptors containing the NR2B subunit compared to those containing the NR2A subunit.

Ro 8-4304 is a non-competitive antagonist at the NMDA receptor

Concentration-response curves for NMDA in rat cultured cortical neurones were carried out in the presence of 0.3, 1 and 3 μM Ro 8-4304 (Figure 3a). NMDA-evoked steady-state currents were reduced in the presence of Ro 8-4304 and the maximum NMDA-evoked currents were concentration-dependently depressed by Ro 8-4304. The apparent microscopic K_D values for the NMDA concentration-response curves were also reduced in the presence of increasing concentrations of Ro 8-4304. Notably, NMDA responses in the presence of Ro 8-4304 exhibited far greater peak to steady-state ratios than control responses (data not shown, but see Figure 5b).

Voltage-independent block of the NMDA receptor by Ro 8-4304

The voltage-dependence of the inhibitory effects of Ro 8-4304 on native NMDA receptors was investigated in rat cultured cortical neurones. The effect of 10 μM Ro 8-4304 on currents elicited by application of 30 μM NMDA at membrane holding potentials of −50 mV and +40 mV was assessed. Application of Ro 8-4304 inhibited steady-state NMDA-evoked currents to 35±3% and 31±2% of control levels at −50 and +40 mV, respectively ($n=5$). Thus, there was no significant difference in the proportion of the steady-state current inhibited by Ro 8-4304 at the two holding potentials ($P>0.35$). Secondly, I/V curves were constructed in the presence and absence of Ro 8-4304. Control I/V curves were constructed by applying NMDA (30 μM) at membrane holding potentials between −80 mV and +40 mV at 20 mV increments. At +40 mV, Ro 8-4304 (10 μM) was applied and once stable responses were achieved a second I/V curve was constructed by applying NMDA, in the continuous presence of Ro 8-4304, at membrane holding potentials between +40 mV and −80 mV (Figure 3b). The inhibition of NMDA currents was not voltage-dependent and the reversal potential of NMDA-induced currents was not altered in the presence of Ro 8-4304.

Activity-dependent block of NMDA receptors by Ro 8-4304

To determine whether Ro 8-4303 exhibited an 'ifenprodil-like' activity-dependent mechanism of antagonism (Kew *et al.*, 1996), we assessed the on-rate time constant of block by Ro 8-4304 in cortical neurones exposed to either 10 or 100 μM NMDA. Once stable steady-state currents were attained, a

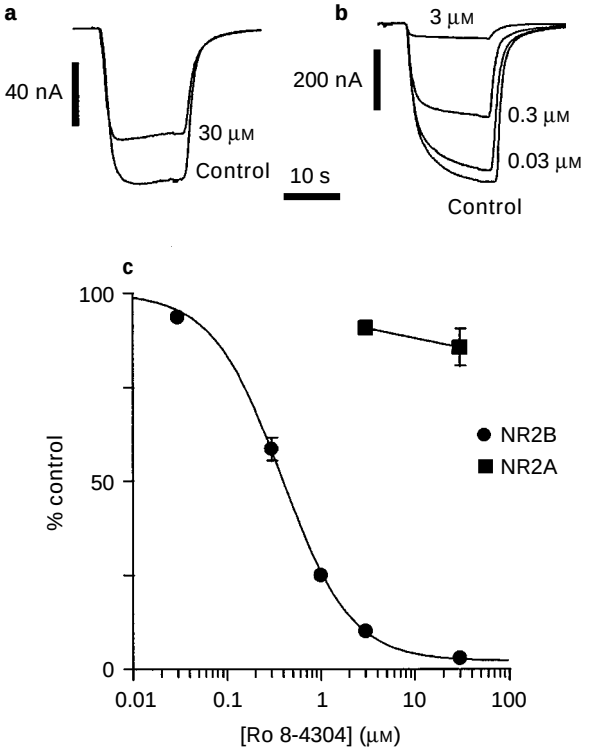

Figure 2 Inhibition of EC_{50} glutamate-activated currents in *Xenopus* oocytes expressing recombinant NMDA receptors. (a) Representative current traces recorded from an oocyte expressing the subunits $NR1_{001}$ and NR2A during activation by 2.7 μM L-glutamate and 0.9 μM glycine. Superimposed traces were recorded before (control) and during the exposure to Ro 8-4304 (30 μM). (b) Currents recorded from an oocyte expressing the $NR1_{001}$ and NR2B subunits before (control) and during the addition of increasing concentrations of Ro 8-4304 (0.03, 0.3 and 3 μM, as indicated). NMDA receptors were activated by 1.3 μM L-glutamate and 0.07 μM glycine. (c) Concentration-inhibitory response relationship. Amplitudes of the current responses in the presence of Ro 8-4304 were expressed as a percentage of the control responses (i.e. pre-Ro 8-4304 response amplitude). Symbols and vertical lines indicate mean values and s.e.mean of the normalized current amplitudes (NR2B, $n=4$ oocytes; NR2A, $n=4-7$ oocytes). The curve fitted to the data for NR2B was calculated from equation 1 with an $IC_{50}=0.38$ μM and Hill coefficient (n_H) = 1.12. The percentage remaining current (ss) = 2.2%.

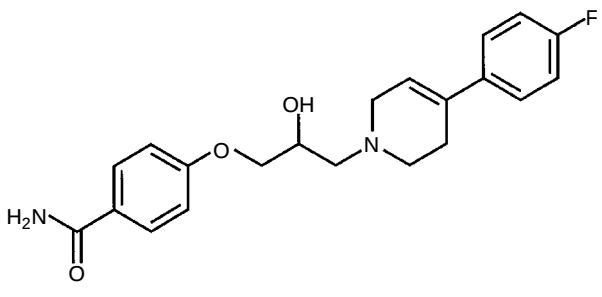

Figure 1 Structure of Ro 8-4304.

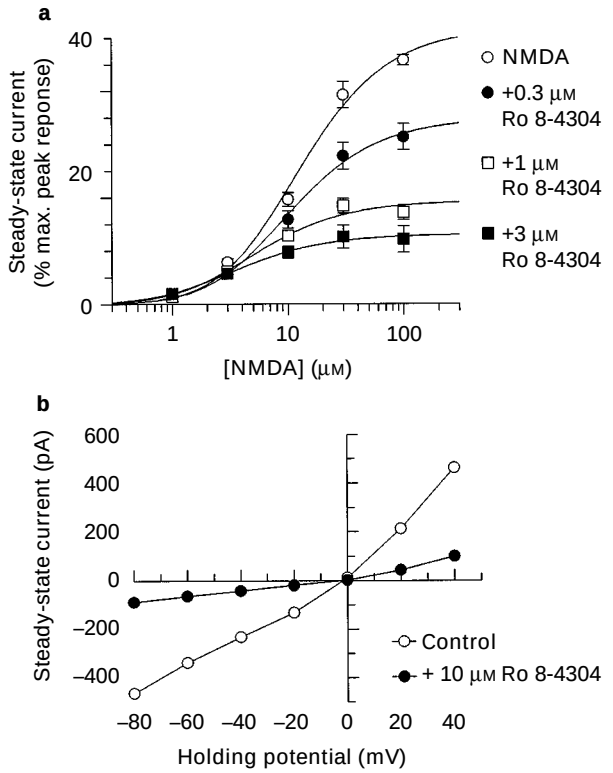

Figure 3 (a) NMDA concentration-response curves in the presence of Ro 8-4304. Concentration-response curves are shown for NMDA alone and in the presence of 0.3 μM, 1 μM and 3 μM Ro 8-4304. Mean steady-state currents and s.e.mean are expressed as a function of the maximum peak NMDA responses derived from a fitted curve of the control peak NMDA concentration-response data for each neurone by use of the two-equivalent-binding-site model (Methods, equation 5) ($n=4$). The figure shows fitted curves obtained with the two-equivalent-binding-site model. Increasing Ro 8-4304 concentration depressed the maximum of the NMDA response curves. In addition, the apparent microscopic K_D value was reduced from 5.5 in the absence of Ro 8-4304 to 4.4, 2.2 and 1.4 μM in the presence of 0.3, 1 and 3 μM Ro 8-4304, respectively. (b) The inhibitory effect of Ro 8-4304 on native NMDA receptors was voltage-independent. *I*-V curves were constructed by applying NMDA (30 μM) at membrane holding potentials between -80 mV and $+40$ mV. At $+40$ mV, Ro 8-4304 (10 μM) was applied and once stable responses were achieved a second *I*-V curve was constructed by applying NMDA, in the continual presence of Ro 8-4304, at holding potentials between $+40$ mV and -80 mV. The figure shows data from a single representative cell. The experiment was repeated 4 times with similar results.

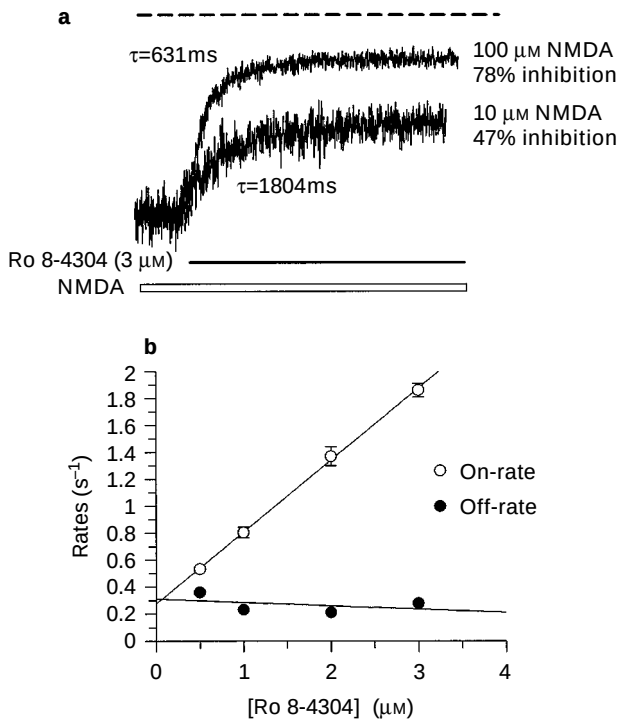

Figure 4 (a) Comparison of the kinetics of inhibition of steady-state inward currents evoked by either 10 or 100 μM NMDA, following fast application of 3 μM Ro 8-4304. The responses have been scaled to the same amplitude to facilitate direct visual comparison (actual steady-state current amplitudes: 10 μM NMDA, 460pA; 100 μM NMDA, 740pA). Single exponential curves were fitted to the digitized data which yielded on-rate time constants for the Ro 8-4304 block of 10 and 100 μM NMDA-evoked currents of 1804 and 631 ms, respectively. Ro 8-4304 inhibited 47 and 78% of the currents evoked by 10 and 100 μM NMDA, respectively. The broken line indicates the baseline current. (b) Kinetic analysis of the block of 100 μM NMDA-evoked steady-state current by Ro 8-4304. Plot of the reciprocal of the on- and off-rate time constants versus Ro 8-4304 concentration. The lines were fitted by linear regression and the points show the means and vertical lines s.e.mean, unless the error lay within the symbol size The apparent association rate increased with Ro 8-4304 concentration, whereas the apparent dissociation rate was independent of antagonist concentration ($n=8$ from 4 cells).

rapid jump was made into a solution containing NMDA + 3 μM Ro 8-4304 (Figure 4a) until stable currents were achieved, at which point a jump was made back into a solution containing NMDA alone. The mean on-rate time constants of Ro 8-4304 block of the 10 and 100 μM NMDA-evoked currents were 1901 ± 72 and 669 ± 33 ms, respectively ($n=16-20$ measurements from 8 cells). Thus, the time constant of block was significantly faster in the presence of the higher NMDA concentration ($P<0.0001$). The mean percentage of the steady-state NMDA-evoked current inhibited by Ro 8-4304 was also significantly greater in 100 μM ($79\pm1\%$) than 10 μM ($47\pm2\%$) NMDA ($P<0.0001$). The mean off-rate time constants of the Ro 8-4304 block of the 10 and 100 μM NMDA-evoked currents were 3412 ± 260 and 4972 ± 165 ms, respectively, also significantly different ($P<0.0001$). From the on- and off- rate time constants, and the resultant forward and reverse rate constants, K_Ds of 3.8 and 0.5 μM were calculated for Ro 8-4304 in 10 and 100 μM NMDA, respectively (see Methods, equations 2–4). Separately, we assessed the on- and off- rate constants of block by Ro 8-4304 at 0.5, 1, 2 and 3 μM of 100 μM NMDA-evoked steady-state currents. A plot of $1/\tau_{on}$ versus Ro 8-4304 concentration was linear over this range (Figure 4b). From the slope of this plot the apparent association rate constant was calculated to be 0.53×10^6 $M^{-1}s^{-1}$ and from the zero y-intercept the apparent dissociation rate constant was estimated to be 0.27 s^{-1}, which was in good agreement with that obtained from the plot of $1/\tau_{off}$ (0.31 s^{-1}). The value of $1/\tau_{off}$ did not alter with changes in Ro 8-4304 concentration. From the apparent association and dissociation rate constants a K_D of 0.5 μM was calculated for Ro 8-4304 in 100 μM NMDA, identical to that already obtained with a single concentration (3 μM) of Ro 8-4304.

To investigate further the apparent increased affinity for Ro 8-4304 in the presence of 100 μM, relative to 10 μM, NMDA, Ro 8-4304 inhibition curves were performed against both 10 and 100 μM NMDA-evoked currents (Figure 5a). Ro 8-4304 discriminates between NR2B and NR2A containing NMDA receptors, exhibiting high and low affinity interactions, respectively (Figure 2). Cortical cultured neurones between 10–14 DIV contain a large proportion of presumed NR2B containing NMDA receptors which bind the NR2B selective antagonist ifenprodil with high affinity (Williams *et al*., 1993; Priestley *et al*., 1994; Kew *et al*., 1996). The present

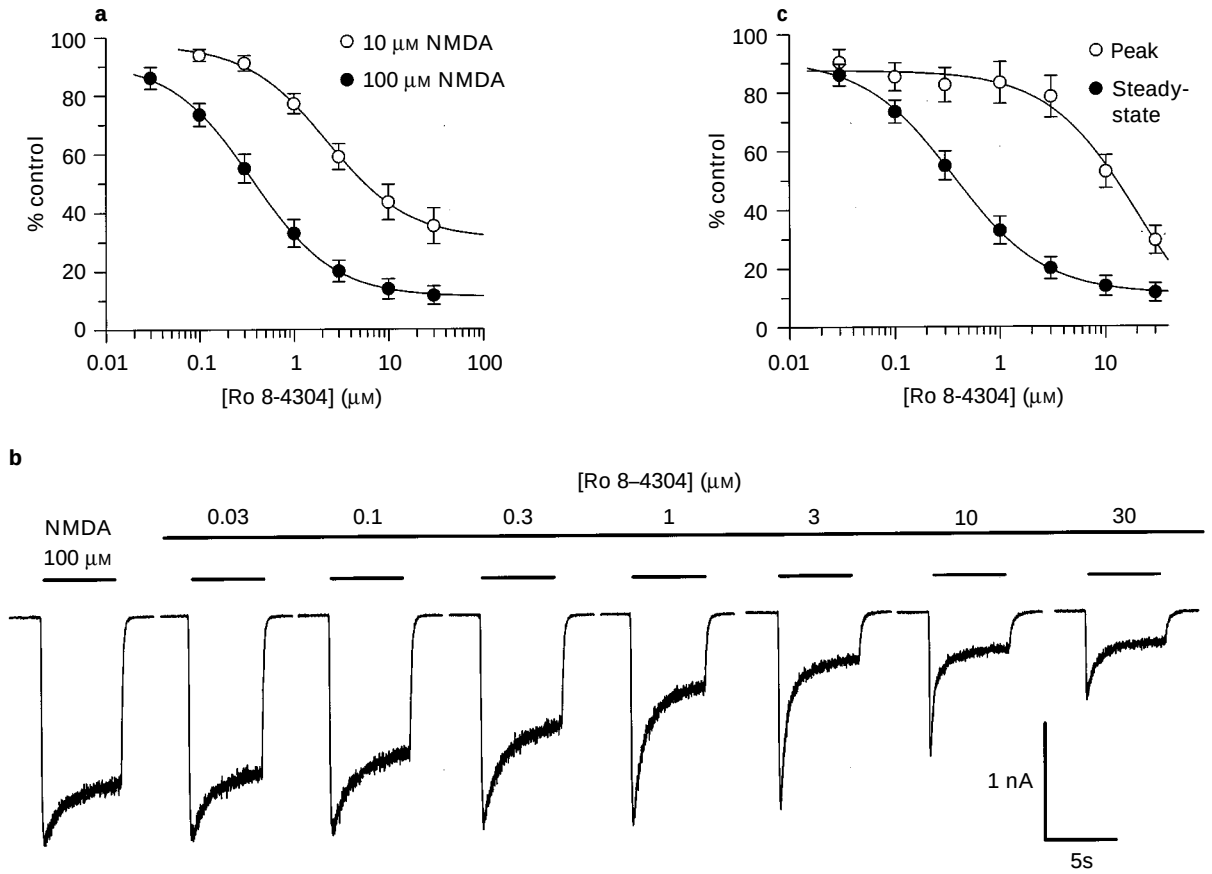

Figure 5 (a) Inhibition curves for the antagonism by Ro 8-4304 of steady-state responses to NMDA at either 10 or 100 μM NMDA. The antagonism of either 10 or 100 μM NMDA responses by increasing concentrations of Ro 8-4304 is expressed as a function of control responses (i.e. pre-Ro 8-4304 response amplitude). The figure shows the fitted curves through the mean data (vertical lines indicate s.e.mean) obtained from 4 neurones, by use of equation 1 with the Hill coefficient fixed to 1, from which IC_{50} values of 2.3 and 0.36 μM Ro 8-4304 were derived for 10 and 100 μM NMDA, respectively. The maximum percentage inhibition of steady-state currents by Ro 8-4304 was also greater for 100 μM, relative to 10 μM, NMDA. (b) Inhibition of NMDA responses by Ro 8-4304. Inward current responses were elicited to 5 s applications of NMDA at 25 s intervals in the presence of increasing concentrations of Ro 8-4304. The figure shows responses obtained from a single cultured cortical neurone. Similar responses were observed in all neurones tested. Note the increased antagonism of steady-state, relative to peak, current at intermediate antagonist concentrations. (c) Inhibition curve for the antagonism by Ro 8-4304 of peak and steady-state 100 μM NMDA-evoked responses. The data for the inhibition of 100 μM NMDA-evoked steady-state currents was taken from (a). Peak NMDA currents are expressed as a function of control responses. Fitted curves through the mean data (vertical lines indicate s.e.mean), by use of equation 1 with the Hill coefficient fixed to 1, yielded IC_{50} values of 0.36 and 20.1 μM for steady-state and peak currents, respectively.

experiments revealed the high affinity interaction only and, therefore, resulted in monophasic inhibition curves. The IC_{50}s of inhibition curves against 10 and 100 μM NMDA were 2.3 and 0.36 μM, respectively, representing an approximate five fold shift, in excellent agreement with the K_Ds calculated previously from the on- and off- rate constants (3.8 and 0.5 μM). Notably, the maximum percentage inhibition of the steady-state current was also greater with 100 than 10 μM NMDA (Figure 5a). Interestingly, when the inhibition of 100 μM NMDA-evoked peak and steady-state currents by Ro 8-4304 was plotted, a clear difference in the apparent affinity of Ro 8-4304 was evident (Figure 5b,c), so that Ro 8-4304 inhibited steady-state currents with an IC_{50} of 0.36 μM and peak currents with an IC_{50} of 20 μM. These observations clearly indicate that the high affinity block of the NMDA receptor by Ro 8-4304 is dependent upon receptor activation.

Effect of Ro 8-4304 on currents evoked by very low NMDA concentrations

Since Ro 8-4304 appeared to exhibit an activity-dependent mechanism of NMDA receptor antagonism analogous to ifenprodil, we investigated the effects of Ro 8-4304 on currents evoked by very low NMDA concentrations which are markedly potentiated in the presence of ifenprodil. Currents evoked by application of 1 μM NMDA were slightly potentiated in the presence of 3–30 μM Ro 8-4304, although only to a maximum of $124 \pm 4\%$ in 10 μM Ro 8-4304 (Figure 6a). Thus, the effect of Ro 8-4304 changed in an NMDA concentration-dependent manner from one of slight potentiation to one of marked inhibition, such that 10 μM Ro 8-4304 slightly potentiated currents evoked by 1 μM NMDA, whilst it markedly inhibited those evoked by 100 μM NMDA in the same neurones (Figure 6b).

Effects of Ro 8-4304 binding on NMDA receptor affinity for glutamate

Ifenprodil binding increases the NMDA receptor affinity for glutamate (Kew *et al*., 1996). This increase in affinity for glutamate-site agonists, revealed by a marked slowing of the current relaxation following removal of glutamate, is likely to mediate the potentiating effects of ifenprodil at low agonist concentrations. Therefore, we investigated the effects of Ro 8-

4304 binding on the kinetics of deactivation of the NMDA receptor following removal of glutamate. Neurones were superfused with control extracellular solution containing 30 μM glycine and a rapid jump was made into an identical solution containing 100 nM glutamate. Once a steady-state current was achieved, a rapid jump was made back into control extracellular solution. These experiments were carried out in both the absence and presence of 10 μM Ro 8-4304. The off-rate time constants of the agonist-evoked currents were then measured. On-rate time constants were not measured in the presence of Ro 8-4304 as the concentration employed (10 μM) is not saturating for the resting state of the NMDA receptor (see Figure 8a, Table 1). Glutamate responses in the presence of Ro 8-4304 were slightly potentiated and exhibited a significant slowing of the current relaxation (Figure 7) which is likely to reflect an increase in receptor affinity for glutamate.

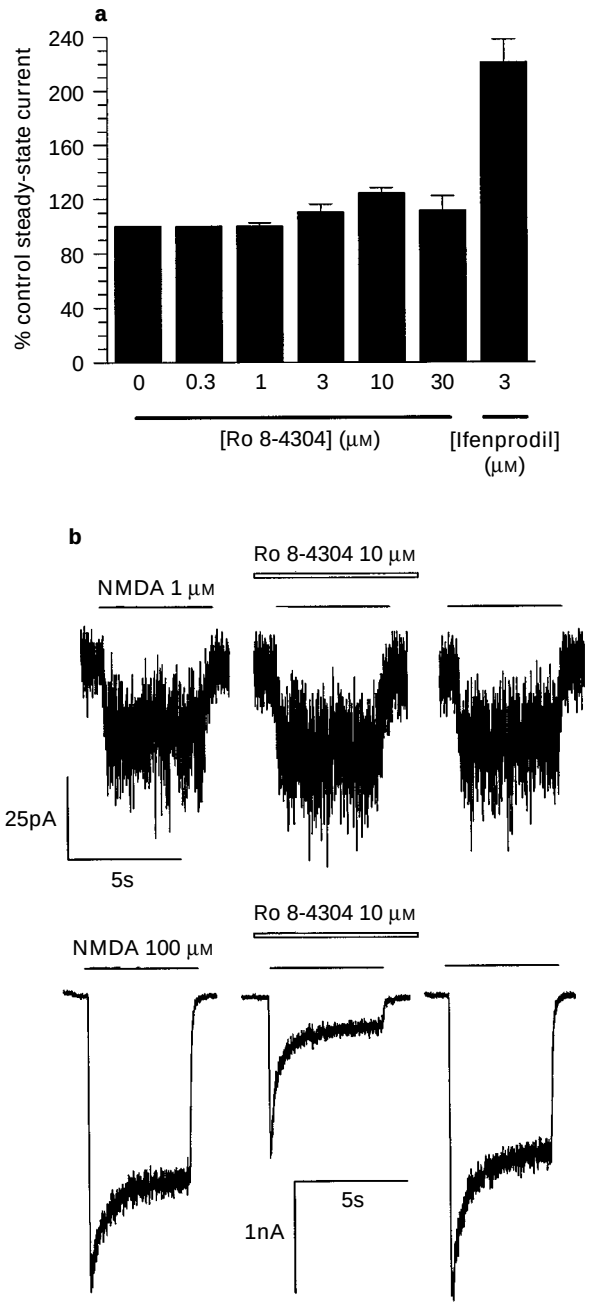

Figure 6 (a) Graph showing the effects of increasing Ro 8-4304 concentration on currents elicited by 1 μM NMDA. Mean data (+s.e.mean) are expressed as a percentage of control steady-state current (i.e. pre-Ro 8-4304 response amplitude) ($n=5$). Ro 8-4304 slightly potentiated currents elicited by 1 μM NMDA to a maximum of 124$\pm$4% at 10 μM Ro 8-4304. The potentiation of 1 μM NMDA responses in the presence of 3 μM ifenprodil is shown for comparative purposes (from Kew *et al*., 1996). (b) The effect of Ro 8-4304 changes from one of slight potentiation to one of inhibition with increasing concentrations of NMDA. Inward current responses were elicited to 5 s applications of either 1 or 100 μM NMDA at 25 s intervals. Once stable responses were achieved, Ro 8-4304 (10 μM) was applied to the neurone until stable responses were again achieved after which Ro 8-4304 was washed off. The figure shows responses obtained from a single cultured cortical neurone, before, during and after Ro 8-4304 exposure for responses to both 1 and 100 μM NMDA. Similar effects were observed in all neurones tested. Ro 8-4304 slightly potentiated currents evoked by 1 μM NMDA and inhibited currents evoked by 100 μM NMDA.

Comparison of the kinetics of binding and unbinding to the NMDA receptor of Ro 8-4304 and ifenprodil

The apparent affinity (IC_{50}s) of ifenprodil and Ro 8-4304 for NR2B containing receptors in *Xenopus* oocytes (Ro 8-4304; 0.39 μM, ifenprodil; 0.25 μM (Trube *et al*., 1996)) and in cultured cortical neurones (high affinity component: Ro 8-4304; 0.36 μM, ifenprodil; 0.17 μM (Kew *et al*., 1996)) were very similar. We, therefore, investigated the kinetics of binding and unbinding of these compounds to both the activated and resting states of the NMDA receptor. To measure the kinetics of the interaction of Ro 8-4304 with the resting state of the NMDA receptor, 0.5 s applications of 10 μM NMDA were made to cortical neurones at 60 s intervals until stable responses were achieved. Ro 8-4304 (10 μM) was then applied to the cell for varying intervals of time before the next NMDA exposure. The inhibition of the subsequent peak NMDA response relative to the preceding control response was plotted against the time period of preincubation with Ro 8-4304. The rate of unblock of the resting state of the NMDA receptor was assessed by repeating this protocol with a fixed 30 s preincubation with 10 μM Ro 8-4304. Following the subsequent NMDA reference application, a second application was made after varying intervals of time and was plotted as a percentage of the reference application against the time period elapsed since Ro 8-4304 removal. The on- and off- rate time constants of inhibition by Ro 8-4304 in the absence of receptor activation were 1.2$\pm$0.2 s ($n=5$) and 2.9$\pm$0.1 s ($n=5$), respectively, which yielded a calculated K_D of 7.4 μM (Table

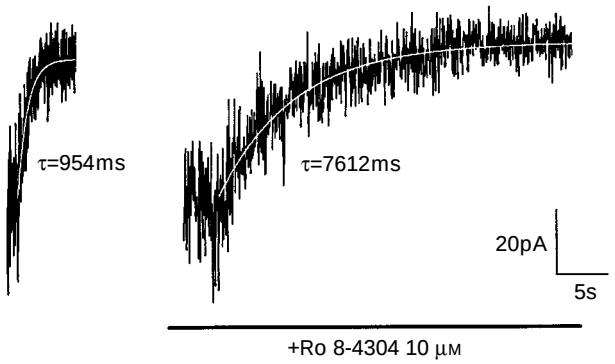

Figure 7 Comparison of glutamate response kinetics in the absence and presence of Ro 8-4304. Current relaxations following removal of L-glutamate (100 nM) in either the absence or presence of Ro 8-4304 are shown for a typical neurone. Exponential curves were fitted to the digitized data (white lines) which yielded off-rate time constants for glutamate of 954 and 7612 ms in the absence and presence or Ro 8-4304, respectively. The glutamate-induced current was slightly potentiated in the presence of Ro 8-4304. Similar results were obtained in all neurones tested ($n=4$).

2). The maximum inhibition was 33±2%. The equivalent on- and off- rate time constants previously determined for 3 μM ifenprodil (Kew *et al*., 1996) were 39 and 61 s respectively, yielding a calculated K_D of 5 μM.

The on- and off- rate time constants for ifenprodil at the activated state of the NMDA receptor were measured, as performed previously for Ro 8-4304, by obtaining a 100 μM NMDA steady-state current and performing a rapid jump into a solution containing NMDA + 3 μM ifenprodil until a stable current was achieved, at which point a jump was made back into a solution containing NMDA alone. The mean on- and off-rate time constants of inhibition were 2.4±0.1 and 50.9±4.4 s, respectively (n = 12 measurements from 5 cells), yielding a calculated K_D of 0.15 μM (Table 2). It should be noted that the long period of NMDA application necessary to obtain these measurements generally resulted in a degree of irreversible run down, with the result that following removal of ifenprodil the response did not recover to its original control level. This run down is likely to result in a small underestimation of the ifenprodil off-rate time constant. The equivalent on- and off- rate time constants for 3 μM Ro 8-4304 were 0.67±0.03 and 4.97±0.16 s, respectively, yielding a calculated K_D of 0.47 μM.

Discussion

In this study we have demonstrated that Ro 8-4304 is a high-affinity, subtype selective NMDA receptor antagonist that exhibits at least a 100 fold higher affinity for recombinant NMDA $NR1_{001}$/NR2B than $NR1_{001}$/NR2A receptors. It was not possible to determine the IC_{50} value for Ro 8-4304 at NR2A-containing receptors due to its limited solubility. However, from the data obtained we would predict a value of at least 100 μM compared with 0.39 μM at NR2B-containing receptors. Ro 8-4304 inhibited NMDA responses elicited in rat cultured cortical neurones in a voltage-independent manner, suggesting that it is unlikely to act as a receptor open channel blocker. Furthermore, the potentiating effects of Ro 8-4304 on small currents evoked by very low concentrations of NMDA are incompatible with the mechanism of action of channel blockers. NMDA concentration-response curves carried out in the presence of Ro 8-4304 exhibited depressed maximum response levels relative to control curves, illustrating that the antagonism is not competitive. Thus, as a subtype selective, non-competitive, non-channel blocker, Ro 8-4304 appears to act by a mechanism similar to that of the prototypic NMDA NR2B subtype selective antagonist, ifenprodil. In this study we have

Table 1 Values of the fitted equilibrium constants

Constant	*Value*
K_1	10 μM
K_2	2.7 μM
K_3	10 μM
K_4	0.70 μM
K_5	0.43 μM
K_6	0.33
K_7	0.054
K_8	1.4
K_9	2.3

The definition of constants K_1-K_9 is given by equations (2)–(12) (Kew *et al*., 1996) and Figure 8a. The value of K_6 was taken from the literature (see Kew *et al*., 1996).

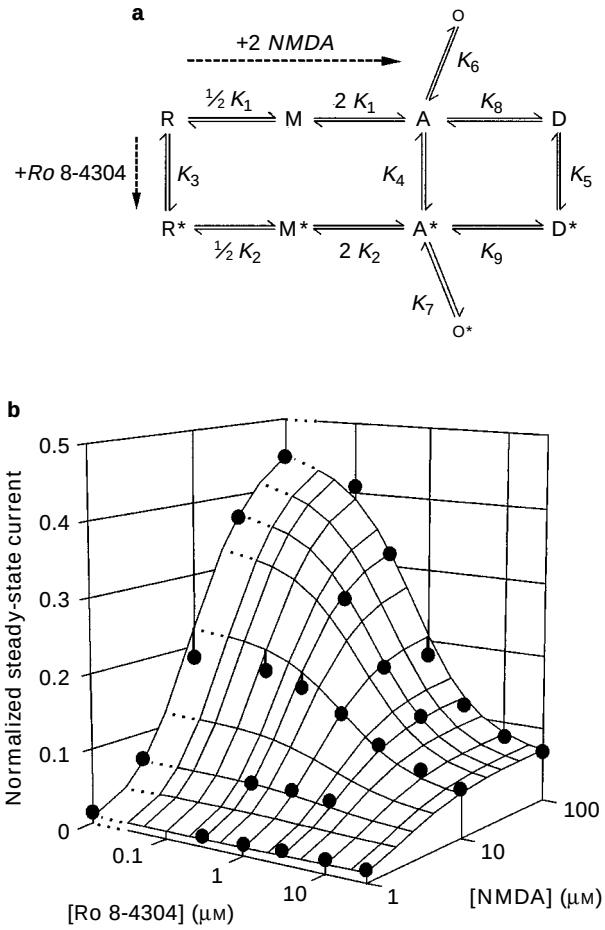

Figure 8 The interaction of Ro 8-4304 and NMDA at the NMDA receptor. (a) Reaction scheme for the interaction of NMDA and Ro 8-4304 at the NMDA receptor channel. Asterisks denote Ro 8-4304-bound states of the channel. One molecule of NMDA is bound to M and M* and two molecules are bound to A and A*. States O and O* are open (conductive) states and all other states are shut. K_1 to K_9 are equilibrium constants, see Kew *et al*. (1996). (b) Three-dimensional plot of the relationship between steady-state current and the concentrations of NMDA and Ro 8-4304. The solid circles are mean values of the measured current amplitudes (4–10 cells per data point from a total of 27 cells). The curved surface (mesh) was calculated as previously described (Kew *et al*., 1996), with the fitted values of K_1-K_9 given in Table 1.

Table 2 Comparison of the rates of Ro 8-4304 and ifenprodil binding and unbinding to the NMDA receptor

		τ_{on} (s)	τ_{off} (s)	k_+† ($M^{-1}s^{-1}$)	k_-† (s^{-1})	k_D† (μM)
Resting state	Ro 8-4304 (10 μM)	1.22	2.88	4.72×10^4	0.348	7.4
	Ifenprodil (3 μM)*	39	61	3.23×10^3	0.016	5.0
Activated state	Ro 8-4304 (3 μM)	0.67	4.97	4.31×10^5	0.201	0.47
	Ifenprodil (3 μM)	2.38	50.87	1.34×10^5	0.020	0.15

†Values derived from the time constants (see Methods, equations 2–4). *From Kew *et al*. (1996).

only employed Ro 8-4304 concentrations within the range of the high affinity interaction with NMDA receptors on cultured cortical neurones, which is likely to reflect its interaction with NMDA receptors containing the NR2B subunit. This distinction is important as it is probable that the mechanism of action of ifenprodil (and thus, possibly also Ro 8-4304) differs at the high and low affinity sites (Reynolds & Miller, 1989; Legendre & Westbrook, 1991; Williams, 1993).

Ro 8-4304 exhibited an activity-dependent block of NMDA receptors, so that the apparent K_Ds, calculated from the measured on- and off- rate time constants of the inhibition of steady-state currents evoked by 10 and 100 μM NMDA, were 3.8 and 0.5 μM, respectively. A plot of the reciprocal of the on- and off- rate time constants of the block of NMDA steady-state currents against a range of Ro 8-4304 concentrations yielded an identical apparent K_D of 0.5 μM for 100 μM NMDA. Steady-state Ro 8-4304 inhibition curves against 10 and 100 μM NMDA-evoked currents yielded IC_{50}s of 2.3 and 0.36 μM, respectively, in very good agreement with the kinetic data. Thus, the apparent affinity of Ro 8-4304 for the NMDA receptor increased in an NMDA-concentration-dependent manner. Interestingly, examination of the inhibition curve against 100 μM NMDA revealed a marked use-dependence of inhibition by Ro 8-4304, so that whilst Ro 8-4304 inhibited steady-state currents with an IC_{50} of 0.36 μM, peak currents were inhibited with an IC_{50} of 20 μM, indicating that Ro 8-4304 exhibits a reduced affinity for the agonist-unbound resting state of the NMDA receptor relative to the agonist-bound activated state. We observed that Ro 8-4304 exhibited very fast binding and unbinding kinetics to the resting state of the NMDA receptor (Table 2) which were compatible with the complete dissociation of Ro 8-4304 from the resting state of the receptor during the 25 s dosing interval. In fact, since Ro 8-4304 is present during both agonist application and wash, dissociation of Ro 8-4304 will proceed, upon removal of NMDA, from a level of receptor occupancy determined by the equilibrium binding affinity of Ro 8-4304 to the NMDA-bound states of the receptor to one determined by the resting state of the receptor. Thus, this IC_{50} value for the peak NMDA responses can be considered as the apparent affinity of Ro 8-4304 for the resting state of the receptor.

In the presence of Ro 8-4304, currents elicited by 1 μM NMDA were slightly potentiated, although only to a maximum of 120% of control levels at 10 μM Ro 8-4304. Importantly, although the potentiation of the current was small in the presence of Ro 8-4304, there was no inhibition of the response. In marked contrast, on the same cells an identical concentration of Ro 8-4304 produced a large inhibition of currents evoked by 100 μM NMDA. Thus, the effect of Ro 8-4304 changed from one of potentiation to one of profound inhibition in an NMDA concentration-dependent manner. Ifenprodil binding to the NMDA receptor increased the receptor affinity for glutamate, an effect which is likely to mediate its potentiating ability on currents evoked by very low NMDA concentrations (Kew *et al*., 1996). The presence of Ro 8-4304 resulted in a significant slowing of the current relaxation following removal of glutamate. It was not possible to obtain an accurate measurement of the glutamate on-rate in the presence of Ro 8-4304 as, due to the limited solubility of the compound, a saturating concentration for the resting state of the receptor could not be achieved. However, the slowing of the current relaxation is likely to reflect an increase in affinity for glutamate of the Ro 8-4304-bound receptor which opposes the inhibitory effect, due to reduced channel opening probability (see below), and mediates the slight potentiating effects of Ro 8-4304 at low NMDA concentrations.

The effects of Ro 8-4304 can be explained by the use of a model that describes the actions of ifenprodil at the NMDA receptor (Kew *et al*., 1996). The model is based on a reaction scheme derived from previously described models of NMDA receptor activation and desensitisation (Benveniste *et al*., 1990; Clements & Westbrook, 1991; Lester & Jahr, 1992) in which the NMDA receptor can reside in five states: a rested state (R), a monoliganded state (M), a double liganded state (A) which can change its state to become an 'open', conductive channel (O), and a desensitized (D) state (Figure 8a). Binding of Ro 8-4304 is suggested to result in a parallel series of Ro 8-4304-bound states, which are identified by asterisks in Figure 8a. The two binding sites for NMDA are assumed to have identical affinities (dissociation constant K_1) without any cooperativity. From this reaction scheme, the relationship between the NMDA-induced steady-state current and the concentrations of NMDA and Ro 8-4304 has been derived (Figure 8, Table 1). Notably, as with ifenprodil, state O* is a conductive state. This is critical to accommodate the slight potentiation of 1 μM NMDA-elicited currents observed in the presence of Ro 8-4304. Surprisingly, the inhibition of NMDA currents in oocytes expressing NR2B was almost complete with only 2.2% remaining current. However, it should be noted that EC_{50} concentrations of both glutamate and glycine were used in these experiments. An allosteric interaction between the glutamate and glycine binding sites on the NMDA receptor exists, such that increasing the affinity for glutamate would be expected to be accompanied by a decrease in affinity for glycine (Benveniste *et al*., 1990; Lester *et al*., 1993). Thus, as Ro 8-4304 binding to the NMDA receptor slows the current relaxation following removal of glutamate, which is likely to reflect an increase in affinity for glutamate, it would be predicted to result in a decrease in affinity for glycine as has been observed with ifenprodil (Legendre & Westbrook, 1991; Ransom, 1991). Thus, inhibition of the NMDA response in the absence of super-saturating concentrations of glycine may result from Ro 8-4304-induced glycine dissociation. The maximum inhibition under these conditions cannot, therefore, be compared directly with that observed in the presence of saturating concentrations of glycine. Additionally, the low level of Ro 8-4304-insensitive, NR2A-containing receptors, in the cortical neurones used in this study, is likely to result in a minor overestimation of receptor open probability in the presence of Ro 8-4304.

From Figure 8 and Table 1 it can be seen that this scheme provides an excellent description of the experimental data. The activity-dependent block of the NMDA receptor is explained by the 14 and 23 fold higher affinities of Ro 8-4304 for the activated (K_4) and desensitized (K_5) states of the NMDA receptor, respectively, relative to the unliganded, resting state (K_3). As such, the antagonism is best described as state-, rather than activity-, dependent. Notably, the value for K_3 (10 μM) is in good agreement with both the apparent equilibrium constant calculated from the inhibition curve of peak 100 μM NMDA currents (20 μM), which provides an estimation of Ro 8-4304 affinity for the resting state of the receptor, as discussed previously, and the calculated affinity for the resting state of the receptor derived from the kinetic measurements (7.4 μM). The value for K_4 (0.7 μM) is, likewise, in good agreement with both the apparent equilibrium constant calculated from the inhibition curve of steady-state 100 μM NMDA currents (0.36 μM) and the equilibrium constants calculated from the kinetics of Ro 8-4304 binding and unbinding to the NMDA receptor during the application of 100 μM NMDA (0.47 μM), which are both likely to reflect Ro 8-4304 binding to the activated state of the receptor. The potentiating effects are

accommodated by the 3–4 fold increase in receptor affinity for NMDA (K_2/K_1) upon Ro 8-4304 binding, so that even though receptor open probability is reduced the increase in the number of agonist-bound receptors results in a small net increase in whole-cell current.

The results obtained for Ro 8-4304 are similar to those obtained previously with ifenprodil (Kew *et al*., 1996). Ro 8-4304 binding results in less of an increase in affinity for glutamate which is likely to explain the reduced potentiation of 1 μM NMDA-elicited currents relative to ifenprodil. The separation in affinity for the resting and double-liganded states is also less for Ro 8-4304 than ifenprodil, and Ro 8-4304 exhibits a somewhat higher preference for the desensitized state relative to the activated state than ifenprodil. Notably, Ro 8-4304 binding and unbinding to both NMDA-bound and resting states of the NMDA receptor appears to be markedly faster than ifenprodil (Table 2). This is surprising since the IC_{50} concentrations at NR2B containing receptors in *Xenopus* oocytes and in cultured cortical neurones (high affinity component only) and the calculated K_D values from the kinetic interactions at both the resting and activated NMDA receptor are very similar. Thus, although the two compounds appear to share a similar mechanism of action at the NMDA receptor and similar affinities, their kinetics are clearly distinct. This distinction illustrates a further feature of this class of compounds that might have important therapeutic implications.

In conclusion, Ro 8-4304 is a novel NR2B selective, non competitive NMDA receptor antagonist that appears to share the mechanism of action previously described for ifenprodil (Kew *et al*., 1996), whilst exhibiting distinctly faster kinetics. The state-dependent mechanism of action of this emerging class of compounds, together with their subunit selectivity, provides an attractive neuropharmacological profile for neuroprotection without side effects.

We would like to thank Dr Günther Fischer and Veronique Graf for the provision of rat cortical neuronal cultures and Urs Humbel and Eva Pflugfelder for expert technical assistance.

References

BEHE, P., STERN, P., WYLLIE, D.J.A., NASSAR, M., SCHOEPFER, R. & COLQUHOUN, D. (1995). Determination of NMDA NR1 subunit copy number in recombinant NMDA receptors. *Proc. R. Soc. Lond.,* **262,** 205–213.

BENVENISTE, M., CLEMENTS, J., VYKLICKY, JR, L. & MAYER, M.L. (1990). A kinetic analysis of the modulation of N-methyl-D-aspartic acid receptors by glycine in mouse cultured hippocampal neurones. *J. Physiol.,* **428,** 333–357.

BERTOCCI, B., MIGGIANO, V., DA PRADA, M., DEMBIC, Z., LAHM, H.W. & MALHERBE, P. (1991). Human catechol-O-methyltransferase: cloning and expression of the membrane-associated form. *Proc. Natl. Acad. Sci. U.S.A.,* **88,** 1416–1420.

BERTRAND, D., COOPER, E., VALERA, S., RUNGGER, D. & BALLIVET, M. (1991). Electrophysiology of neuronal nicotinic acetylcholine receptors expressed in Xenopus oocytes following nuclear injection of genes or cDNAs. In *Electrophysiology and Microinjection (Methods in Neurosciences*), Vol 4. ed. Conn, P.M. pp. 174–193. San Diego: Academic Press.

CARTER, C.J., LLOYD, K.G., ZIVKOVIC, B. & SCATTON, B. (1990). Ifenprodil and SL 82.0715 as cerebral antiischemic agents. III. Evidence for antagonistic effects at the polyamine modulatory site within the N-methyl-D-aspartate receptor complex. *J. Pharmacol. Exp. Ther.,* **253,** 475–482.

CHAZOT, P.L., COLEMAN, S.K., CIK, M. & STEPHENSON, F.A. (1994). Molecular characterization of N-methyl-D-aspartate receptors expressed in mammalian cells yields evidence for the coexistence of three subunit types within a discrete receptor molecule. *J. Biol. Chem.,* **269,** 24403–24409.

CLEMENTS, J.D. & WESTBROOK, G.L. (1991). Activation kinetics reveal the number of glutamate and glycine binding sites on the N-Methyl-D-aspartate receptor. *Neuron,* **7,** 605–613.

FERRER-MONTIEL, A.V. & MONTAL, M. (1996). Pentameric subunit stoichiometry of a neuronal glutamate receptor. *Proc. Natl. Acad. Sci. U.S.A.,* **93,** 2741–2744.

GALLAGHER, M.J., HUANG, H., PRITCHETT, D.B. & LYNCH, D.R. (1996). Interactions between ifenprodil and the NR2B subunit of the N-methyl-D-aspartate receptor. *J. Biol. Chem.,* **271,** 9603–9611.

GOTTI, B., DUVERGER, D., BERTIN, J., CARTER, C., DUPONT, R., FROST, J., GAUDILLIERE, B., MACKENZIE, E.T., ROUSSEAU, J., SCATTON, B. & WICK, A. (1988). Ifenprodil and SL 82.0715 as cerebral anti-ischemic agents. I. Evidence for efficacy in models of focal cerebral ischemia. *J. Pharmacol. Exp. Ther.,* **247,** 1211–1221.

GRAHAM, D., DARLES, G. & LANGER, S.Z. (1992). The neuroprotective properties of ifenprodil, a novel NMDA receptor antagonist, in neuronal cell culture toxicity studies. *Eur. J. Pharmacol.,* **226,** 373–376.

ISHII, T., MORIYOSHI, K., SUGIHARA, H., SAKURADA, K., KADOTANI, H., YOKOI, M., AKAZAWA, C., SHIGEMOTO, R., MIZUNO, N., MASU, M. & NAKANISHI, S. (1993). Molecular characterization of the family of the N-methyl-D-aspartate receptor subunits. *J. Biol. Chem.,* **268,** 2836–2843.

JACKSON, A. & SANGER, D.J. (1988). Is the discriminative stimulus produced by phencyclidine due to an interaction with N-methyl-D-aspartate receptors? *Psychopharmacology,* **96,** 87–92.

KASHIWAGI, K., FUKUCHI, J.-I., CHAO, J., IGARASHI, K. & WILLIAMS, K. (1996). An aspartate residue in the extracellular loop of the N-methyl-D-aspartate receptor controls sensitivity to spermine and protons. *Mol. Pharmacol.,* **49,** 1131–1141.

KEMP, J.A. & KEW, J.N.C. (1998). NMDA receptor antagonists. In *Receptor Based Drug Design*. ed. Leff, P. New York: Marcel Dekker (in press).

KEW, J.N.C., TRUBE, G. & KEMP, J.A. (1996). A novel mechanism of activity-dependent NMDA receptor antagonism describes the effect of ifenprodil in rat cultured cortical neurones. *J. Physiol.,* **497,** 761–772.

KUTSUWADA, T., KASHIWABUCHI, N., MORI, H., SAKIMURA, K., KUSHIYA, E., ARAKI, K., MEGURO, H., MASKAI, H., KUMANISHI, T., ARAKAWA, M. & MISHINA, M. (1992). Molecular diversity of the NMDA receptor channel. *Nature,* **358,** 36–41.

LAURIE, D.G. & SEEBURG, P.H. (1994). Regional and developmental heterogeneity in splicing of the rat brain NMDAR1 mRNA. *J. Neurosci.,* **14,** 3180–3194.

LAURIE, D.J., PUTZKE, J., ZIEGLGÄNSBERGER, W., SEEBURG, P.H. & TOLLE, T.R. (1995). The distribution of splice variants of the NMDAR1 subunit mRNA in the adult rat brain. *Mol. Brain Res.,* **32,** 94–108.

LEGENDRE, P. & WESTBROOK, G.L. (1991). Ifenprodil blocks N-methyl-D-aspartate receptors by a two-component mechanism. *Mol. Pharmacol.,* **40,** 289–298.

LESTER, R.A.J. & JAHR, C.E. (1992). NMDA channel behaviour depends on agonist affinity. *J. Neurosci.,* **12,** 635–643.

LESTER, R.A.J., TONG, G. & JAHR, C.E. (1993). Interactions between the glycine and glutamate binding sites of the NMDA receptor. *J. Neurosci.,* **13,** 1088–1096.

LUO, J., WANG, Y., YASUDA, R.P., DUNAH, A.W. & WOLFE, B.B. (1997). The majority of N-methyl-D-aspartate receptor complexes in adult rat cerebral cortex contain at least three different subunits (NR1/NR2A/NR2B). *Mol. Pharmacol.,* **51,** 79–86.

MCBAIN, C.J. & MAYER, M.L. (1994). N-methyl-D-aspartic acid receptor structure and function. *Physiol. Rev.,* **74,** 723–760.

MEGURO, H., MORI, H., ARAKI, K., KUSHIYA, E., KUTSUWADA, T., YAMAZAKI, M., KUMANISHI, T., ARAKAWA, M., SAKIMURA, K. & MISHINA, M. (1992). Functional characterization of a heteromeric NMDA receptor channel expressed from cloned cDNAs. *Nature,* **357,** 70–74.

MÖCKEL, G. & FISCHER, G. (1994). Vulnerability to excitotoxic stimuli of cultured rat hippocampal neurons containing the calcium-binding proteins calretinin and calbindin D_{28k}. *Brain Res.,* **648,** 109–120.

MONYER, H., BURNASHEV, N., LAURIE, D.J., SAKMANN, B. & SEEBURG, P.H. (1994). Developmental and regional expression in the rat brain and functional properties of four NMDA receptors. *Neuron,* **12,** 529–540.

MONYER, H., SPRENGEL, R., SCHOEPFER, R., HERB, A., HIGUCHI, M., LOMELI, H., BURNASHEV, N., SAKMANN, B. & SEEBURG, P.H. (1992). Heteromeric NMDA receptors: molecular and functional distinction of subtypes. *Science,* **256,** 1217–1221.

PERRAULT, G., MOREL, E., SANGER, D.G. & ZIVKOVIC, B. (1989). Comparison of the pharmacological profiles of four NMDA antagonists, ifenprodil, SL 82.0715, MK-801 and CPP, in mice. *Br. J. Pharmacol.,* **97,** 580P.

PRIESTLEY, T., OCHU, E. & KEMP, J.A. (1994). Subtypes of NMDA receptor in neurones cultured from rat brain. *NeuroReport,* **5,** 1763–1765.

RANSOM, R.W. (1991). Polyamine and ifenprodil interactions with the NMDA receptor's glycine site. *Eur. J. Pharmacol.,* **208,** 67–71.

REYNOLDS, I.J. & MILLER, R.J. (1989). Ifenprodil is a novel type of N-methyl-D-aspartate receptor antagonist: interaction with polyamines. *Mol. Pharmacol.,* **36,** 758–765.

SHENG, M., CUMMINGS, J., ROLDAN, L.A., JAN, Y.N. & JAN, L.Y. (1994). Changing subunit composition of heteromeric NMDA receptors during development of rat cortex. *Nature,* **368,** 144–147.

SIGEL, E., BAUR, R. & MALHERBE, P. (1994). Protein kinase C transiently activated heteromeric N-methyl-D-aspartate receptor channels independent of the phosphorylatable C-terminal splice domain and of consensus phosphorylation sites. *J. Biol. Chem.,* **269,** 8204–8208.

TRUBE, G., EHRHARD, P., MALHERBE, P. & HUBER, G. (1996). The selectivity of RO 25-6981 for NMDA receptor subtypes expressed in Xenopus oocytes. *Soc. Neurosci. Abstr.,* 693.4.

WAFFARD, K.A., BAIN, C.J., LE BOURDELLES, B., WHITING, P.J. & KEMP, J.A. (1993). Preferential co-assembly of recombinant NMDA receptors composed of three different subunits. *NeuroReport,* **4,** 1347–1349.

WILLIAMS, K. (1993). Ifenprodil discriminates subtypes of the N-methyl-D-aspartate receptor: selectivity and mechanisms at recombinant heteromeric receptors. *Mol. Pharmacol.,* **44,** 851–859.

WILLIAMS, K., KASHIWAGI, K., FUKUCHI, J.-I. & IGARASHI, K. (1995). An acidic amino acid in the N-methyl-D-aspartate receptor that is important for spermine stimulation. *Mol. Pharmacol.,* **48,** 1087–1098.

WILLIAMS, K., RUSSELL, S.L., SHEN, Y.M. & MOLINOFF, P.B. (1993). Developmental switch in the expression of NMDA receptors occurs in vivo and in vitro. *Neuron,* **10,** 267–278.

ZUKIN, R.S. & BENNETT, M.V.L. (1995). Alternatively spliced isoforms of the NMDAR1 receptor subunit. *Trends Neurosci.,* **18,** 306–313.

(Received August 26, 1997
Accepted October 28, 1997)